Eur Biophys J (2005) 34: 881–889
DOI 10.1007/s00249-004-0458-4

ARTICLE

**Antonio Cupane · Marco Cammarata
Lorenzo Cordone · Maurizio Leone · Eugenio Vitrano
Niklas Engler · Fritz Parak**

Spectral broadening of the Soret band in myoglobin: an interpretation by the full spectrum of low-frequency modes from a normal modes analysis

Received: 6 September 2004 / Revised: 9 December 2004 / Accepted: 17 December 2004 / Published online: 15 March 2005

Abstract In this work the temperature dependence of the Soret band line shape in carbonmonoxy myoglobin is re-analyzed by using both the full correlator approach in the time domain and the frequency domain approach. The new analyses exploit the full density of vibrational states of carbonmonoxy myoglobin available from normal modes analysis, and avoid the artificial division of the entire set of vibrational modes coupled to the Soret transition into "high-frequency" and "low-frequency" subsets; the frequency domain analysis, however, makes use of the so-called short-times approximation, while the time domain one avoids it. Time domain and frequency domain analyses give very similar results, thus supporting the applicability of the short-times approximation to the analysis of hemeprotein spectra; in particular, they clearly indicate the presence of spectral heterogeneity in the Soret band of carbonmonoxy myoglobin. The analyses also show that a temperature dependence of the Gaussian width parameter steeper than the hyperbolic cotangent law predicted by the Einstein harmonic oscillator and/or a temperature dependence of inhomogeneous broadening are not sufficient to obtain quantitative information on the magnitude of anharmonic contributions to the iron–heme plane motion. However, the dependence of the previous two quantities may be used to obtain semiquantitative information on the overall coupling of the Soret transition to the low-frequency modes and therefore on the dynamic properties of the heme pocket in different states of the protein.

A. Cupane (✉) · M. Cammarata · L. Cordone
M. Leone · E. Vitrano
Istituto Nazionale per la Fisica della Materia (INFM),
Dipartimento di Scienze Fisiche e Astronomiche
dell'Università, Via Archirafi, 36,
90123 Palermo, Italy
E-mail: cupane@fisica.unipa.it

N. Engler · F. Parak
Physik-Abteilung E17, Technische Universität München,
85747 Garching, Germany

Keywords Myoglobin · Optical spectroscopy · Normal modes analysis

Introduction

In previous papers (Di Pace et al. 1992, Cupane et al. 1995) a method was developed for analyzing the line shape of the Soret band in hemeproteins. One of the relevant parameters obtained from the fitting procedure was the Gaussian broadening, whose squared value (σ^2) was used by the authors as a marker of the extent of mean square fluctuations of the iron with respect to the heme plane (Melchers et al. 1996). In the fittings of the absorption line shape, performed in the frequency domain, a subdivision of the entire set of vibrational normal modes coupled to the electronic transition into two subsets was used:

1. "High-frequency modes", not populated in the temperature range investigated.
2. "Low-frequency modes", considered as a thermal bath whose population varies as a function of temperature; coupling to low-frequency modes was treated within the so-called short-times approximation.

The temperature dependence of the Gaussian thermal broadening (σ) was considered to arise from the coupling of the electronic transition with low-frequency modes. By considering the bath of low-frequency modes within the Einstein approximation it was inferred that the temperature dependence of σ^2 should have obeyed the well-known hyperbolic cotangent law which describes the mean square displacement of a single quantized harmonic oscillator. In view of the coupling of the iron vibration with the Soret (B) band ($\pi \rightarrow \pi^*$ electronic transition), deviations from hyperbolic cotangent behavior were interpreted as implying the presence of nonharmonic contributions to the motion

of the iron with respect to the heme plane. This interpretation was also supported by experimental studies on various metal octaethylporphyrins and heme complexes (Leone et al. 1994, Cupane and coworkers 1996, 1998).

The previously described approach can be criticized in two respects. First of all, the validity of the short-times approximation as applied to modes having frequency of the same order of k_BT/hc can be questioned (although its applicability has been supported with numerical examples by Chan and Page 1984). Second, the division of vibrational modes coupled to the transition into high-frequency, temperature-independent, and low-frequency ones is not fully appropriate. Indeed, the number of modes to be considered as low frequency increases by increasing the temperature with the simultaneous decrease of the number of high-frequency ones. This effect, which may be relevant in determining the $\sigma^2(T)$ values, was not taken into account in the papers mentioned, owing to the lack of knowledge of the spectrum of the low-frequency modes in myoglobin.

In this paper we revisit the fitting of the Soret band line shape in the temperature range 20–300 K for carbonmonoxy myoglobin (MbCO) using two alternative approaches:

1. A modified frequency domain approach in which the short-times approximation is still used, but in which the temperature-dependent conversion from a high-frequency to a low-frequency subset is explicitly taken into account.
2. The full correlator approach, in the time domain, in which the short-times approximation is avoided.

Both approaches rely on the normal modes analysis of MbCO, which gives the whole data set of vibrational normal modes of the protein and solvent system (Melchers et al. 1996).

The aim of the paper is to compare the two methods, with particular attention to the applicability of the short-times approximation to the analysis of hemeprotein spectra, and to ascertain whether reliable information on protein dynamics and anharmonicity can be obtained from the analysis of the temperature dependence of the absorption spectra.

Theory

There are two equivalent ways to calculate the absorption band shape of an electronic transition coupled to the vibrations of surrounding atoms. Chan and Page (1983, 1984) described the time-correlator approach which was used by Champion's group (Schomacker and Champion 1986, Srajer et al. 1986) to model the band shape of ferrous cytochrome c, of MbCO and of deoxymyoglobin. Since the short-times approximation has been formulated in this framework and is essential for the definition of the terms high-frequency modes and low-frequency modes, we briefly summarize their results before returning to the formalism in the frequency domain developed by Cupane et al. (1995).

The absorption coefficient μ as a function of the frequency of the incident light ω is given by

$$\mu(\omega) = C \cdot \omega \cdot \mathrm{Im}\Phi(\omega), \tag{1}$$

where C is a constant and

$$\Phi(\omega) = i \cdot \int_0^\infty \exp\left(i\omega t - \Gamma t\right) \cdot \eta(t)\mathrm{d}t \tag{2}$$

describes the decay of the excited state with width Γ. The time correlator $\eta(t)$ contains the coupling of the pure electronic transition with frequency ω_0 and the vibrations with frequencies ω_j and is given by

$$\eta(t) = \exp\left(-i\omega_0 t\right) \exp\left\{-\sum_j S_j\left[\left(2\langle n_j\rangle + 1\right)\left(1-\cos\omega_j t\right) + i\sin\omega_j t\right]\right\}. \tag{3}$$

The S_j are the electron–nuclear coupling strengths and $<n_j>$ are the Bose–Einstein factors for the different vibrations. The formalism used in Eqs. 1, 2 and 3 is derived under the assumption of a single electronic excited state, linear electron–phonon coupling, harmonic approximation for the vibrations, and adiabatic and Condon approximations. Use of Eqs. 1, 2 and 3 for the analysis of absorption spectra of hemeproteins, however, requires knowledge of the full set of vibrational modes coupled to the electronic transition (ω_j) and of their coupling strengths (S_j). A simplified expression can be obtained on the basis of the following considerations. The integral in Eq. 2 is the Fourier transform of a function decaying with Γ . Therefore, for modes having a prefactor $\sum S_j\left(2\langle n_j\rangle + 1\right) \gg 1$, only short times contribute to Eq. 2. Accordingly, $\cos\omega t$ and $\sin\omega t$ can be expanded up to order t^2 . This condition is equivalent to highly excited modes, which correspond to low frequencies, denoted by ω_l. Thus, Eq. 3 can be rewritten as

$$\eta(t) = \exp\left[-it\left(\omega_0 + \sum_l S_l\omega_l\right)\right]\exp\left(-\frac{1}{2}\sigma^2 t^2\right) \exp\left\{-\sum_h S_h[(2\langle n_h\rangle + 1)(1-\cos\omega_h t) + i\sin\omega_h t]\right\}. \tag{4}$$

The high- and low-frequency modes are denoted by the subscripts h and l respectively, and

$$\sigma^2 = \sum_l S_l(2\langle n_l\rangle + 1)\omega_l^2. \tag{5}$$

Within this short-times approximation, the coupling with low-frequency modes leads to a temperature-independent shift of the transition frequency and to an additional decay of the time correlator, whose Fourier

transform causes a Gaussian broadening of the band. Chan and Page (1984) have illustrated the validity of the short-times approximation with numerical examples. One important feature, put forward by these simulations, concerns the relevance of dephasing among low-frequency modes. Modeling of the line shape in terms of Eqs. 1, 2 and 3 with only a single low-frequency mode leads to unsuitable results, as the decay of the time correlator is not fast enough; a multitude of modes with different frequencies is always needed to get a meaningful model. We stress, however, that if the entire set of normal modes and of their coupling strengths to the electronic transition is known, the full time correlator (Eq. 3) can be used, avoiding the short-times approximation.

Cupane et al. (1995) derived essentially the same relations. The most important difference is the development of the theory in the frequency domain rather than in the time domain. Cupane et al. (1995) expressed the absorption in terms of a series of Lorentzians, weighted by the thermal population of the vibrational states in the electronic ground state. By expressing the Lorentzians as their Fourier transforms they reached, after some manipulation, the same result described earlier (Eqs. 2, 3). Going back to the frequency domain, a fit of the spectra in terms of a convolution of Lorentzians with a Gaussian is performed (we keep the notations for frequencies and coupling constants of each formalism, to facilitate the comparison with respective publications).

$$\mu(\nu) = M\nu[L(\nu) \otimes G(\nu)], \tag{6}$$

where

$$L(\nu) = \sum_{m_1, m_2 \ldots m_{Nh}} \left\{ \left[\prod_{j=1}^{N_h} \frac{\mathrm{e}^{-S_j} S_j^{m_j}}{m_j!} \right] \times \frac{\Gamma(T)}{\left[\nu - \nu_0(T) - \sum_{j=1}^{N_h} m_j \nu_j \right]^2 + \Gamma^2(T)} \right\} \tag{7}$$

and

$$G(\nu) = \frac{1}{\sigma(T)} \exp\left[-\frac{\nu^2}{2\sigma^2(T)} \right]. \tag{8}$$

In Eq. 7, Γ is the Lorentzian width, determined by the lifetime of the excited state; moreover the quadratic electron–phonon coupling (i.e., the change in vibrational frequencies from the ground state to excited electronic states) is not considered. The homogeneous (Lorentzian) width—parameter Γ in Eq. 7—is left as a free parameter in the spectral fittings. For MbCO, typical Γ values are in the range 230–260 cm^{-1} and the temperature dependence is very weak (Di Pace et al. 1992, Cupane et al.1995). Moreover, as shown in Eq. 7, Γ is assumed to be the same for all vibronic transitions; this assumption, commonly used in the literature (Schomacker and Champion 1986, Schweitzer-Stenner and Bigman 2001), is necessary to avoid a large number of fitting parameters and is justified a posteriori by the good quality of the fittings (Figs. 3, 7). The contributions of different high frequency vibrational modes are weighted by a factor, which contains the linear coupling constants S_j.

These last quantities are a measure of the linear coupling of the vibrational mode of frequency ν_j to the electronic transition (i.e., of the shift of nuclear equilibrium positions following the electronic excitation). The frequency values for the high-frequency modes (ν_j) are taken from independent resonance Raman measurements. The Gaussian broadening is given by (Di Pace et al. 1992)

$$\sigma^2(T) = \sum_{j=1}^{N_l} S_j \nu_j^2 coth\left(\frac{h\nu_j}{2k_B T} \right). \tag{9}$$

To reduce the number of parameters, a single mode representing the bath of low-frequency normal modes (harmonic Einstein approximation) was used by Cupane et al. (1995); thus, Eq. 9 reduces to

$$\sigma^2(T) = N_l \langle S \rangle \langle \nu \rangle^2 coth\left(\frac{h\langle \nu \rangle}{2k_B T} \right), \tag{10}$$

where N_l is the number of low-frequency modes, $< S >$ is the mean coupling constant and $< \nu >$ is the mean frequency. Note that Eqs. 5 and 10 are identical, since $2\langle n \rangle + 1 = \coth(h\langle \nu \rangle / 2k_B T)$.

It should also be noted that in analyzing the temperature dependence of the Gaussian broadening of the Soret bands of hemeproteins, a temperature-independent term, σ_{inh}, is added to Eq. 10, to take into account the presence of spectral heterogeneity arising from conformational substates (Cupane et al. 1995).

Results and discussion

Frequency domain approach

In previous publications (Cupane et al. 1995) the experimentally determined temperature dependence of the Soret band of, for example, MbCO was analyzed in the following way:

1. The high-frequency modes significantly coupled to the electronic transition were selected from resonance Raman data (Bangcharoenpaurpong et al. 1984). For MbCO these are at 350, 676, 1,100 and 1,374 cm^{-1}; all modes of frequency less than 300 cm^{-1} were considered in the low-frequency bath.
2. The Soret band profile measured at various temperatures was fitted to Eqs. 6, 7 and 8, thus obtaining the σ^2 values.
3. The dependence of σ^2 on temperature was analyzed by considering an average mode as representative of the bath of low-frequency modes (harmonic Einstein

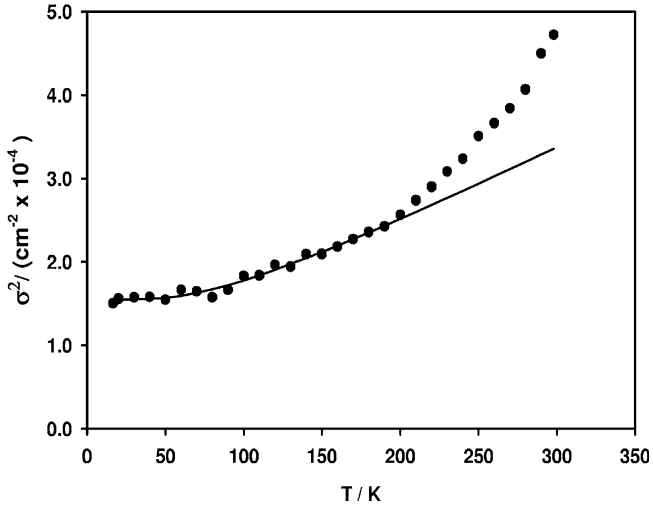

Fig. 1 Temperature dependence of σ^2 obtained by fitting the Soret spectra of carbonmonoxy myoglobin (*MbCO*) in terms of Eqs. 6, 7 and 8. The *continuous line* is a fit of σ^2 values, in the temperature range 20–160 K, in terms of Eq. 10 (harmonic Einstein approximation)

approximation, see Eq. 10). Typical results of such an analysis are reported in Fig. 1.

4. Deviations from the hyperbolic cotangent law, evident in Fig. 1, were interpreted as arising from non-harmonic contributions to the motions of the iron with respect to the heme plane.

It is important to note that the dependence of σ^2 on temperature is brought about by a twofold effect:

1. The contribution of each individual low-frequency mode, as described by the sum of hyperbolic cotangents in Eq. 9. Note that, strictly speaking, the sum of hyperbolic cotangent functions with different arguments is not a hyperbolic cotangent function.
2. The increase, with temperature, of the number of modes that must be considered low frequency, accompanied by an analogous and simultaneous decrease of the number of high-frequency modes. This second effect was not considered in the approach used in the aforementioned papers.

To overcome this problem, we decided to avoid (1) the artificial division between high- and low-frequency modes and (2) the assumption of a mean bath mode for the low-frequency subset. We used, instead, the full density of vibrational modes shown in Fig. 2, obtained from the normal modes analysis of MbCO and deoxymyoglobin, including the 170 crystallographically visible water molecules reported by Melchers et al. (1996). The crucial point for the new approach is to discriminate whether a given mode, at a given temperature, has to be taken into account as a low-frequency or as a high-frequency one. In fact, since the short-times approximation is valid only for modes thermally excited, at a given temperature only modes below a certain frequency, ν_{max}, contribute to the Gaussian broadening. The problem is that ν_{max} increases with temperature; from energy considerations we can take

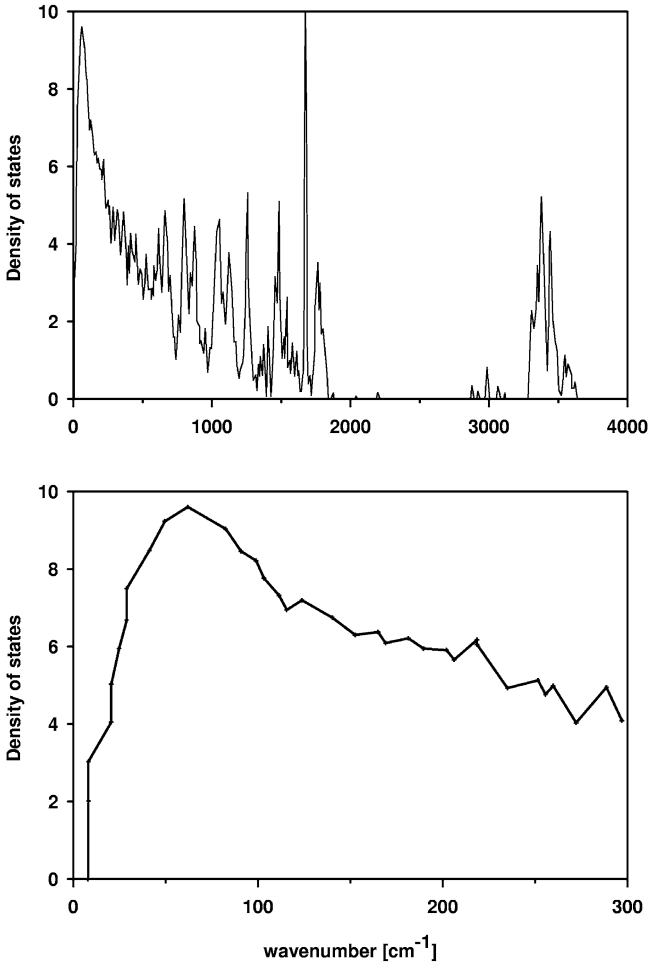

Fig. 2 Calculated density of vibrational states spectrum of MbCO with 170 crystal water molecules (reported from Melchers et al. 1996). *Upper panel* The whole spectrum. *Lower panel* The relevant low-frequency part. For comparison note that $T = 300$ K corresponds to approximately 210 cm^{-1}

$\nu_{max} = k_B T/hc$ as the upper frontier of the low-frequency subset. We modeled the effect of the ν_{max} temperature dependence, in the analysis of the temperature dependence of σ^2, by multiplying the coupling constant of each low-frequency vibrational mode at frequency ν_j (S_j; see Eq. 9) by a "switch function":

$$f(\nu_j, T) = \frac{1}{\exp\left[\left(\nu_j - k_B T/hc\right)/\Delta\nu\right] + 1}. \qquad (11)$$

The function $f(\nu_j,T)$, which is used in this context only for practical purposes, is 1 below $\nu_{max} = k_B T/hc$ and 0 above it, with a smooth but rapid fall off in the interval $|\nu - \nu_{max}| \leqslant \Delta\nu$, which was set to $1 cm^{-1}$. Equation 11 describes the fact that, at temperature T, a vibrational mode has to be considered in the low-frequency subset only if its frequency $\nu_j < \nu_{max}$. Of course, when by lowering the temperature the condition $\nu_j < \nu_{max}$ is no longer fulfilled, the mode must be shifted from the low-frequency to the high-frequency subset; this can be done by multiplying the coupling constant S_j in Eq. 7 by the function $[1 - f(\nu_j,T)]$.

Accordingly, the new analysis proceeded as follows:

1. We first divided the vibrational modes frequency range 0–220 cm^{-1} into 11 intervals of 20 cm^{-1} each; the average frequency of the interval is assigned to each interval and the number of modes in the interval is calculated from the density of vibrational states in Fig. 2. To this set, four high-frequency modes taken from resonance Raman spectroscopy, i.e., modes at 350, 676, 1,100 and 1,374 cm^{-1}, are added. Note that these modes are to be considered as high-frequency modes in the entire temperature range investigated ($k_B T/hc \approx 215$ cm^{-1} at 300 K).
2. Spectra at various temperatures are analyzed with Eqs. 6, 7 and 8, in which, however, Eq. 7 is replaced by

$$L(\nu) = \sum_{m_1, m_2 \ldots m_{15}} \left\{ \left[\prod_{j=1}^{15} \frac{e^{-S_j \cdot [1 - f(\nu_j, T)]} S_j^{m_j} \cdot [1 - f(\nu_j, T)]}{m_j!} \right] \cdot \times \frac{\Gamma(T)}{\left[\nu - \nu_0(T) - \sum_{j=1}^{15} m_j \nu_j \right]^2 + \Gamma(T)^2} \right\} \quad (12)$$

Owing to the lack of information on the coupling constants of low-frequency modes ($j = 5$–15 in the sum of Eq. 12), we used one single value for the coupling constant S (unspecific coupling of the 11 low-frequency modes). [1]At variance, the values of the coupling constants for the four modes at 350, 676, 1,100 and 1,374 cm^{-1} ($j = 1$–4 in the sum of Eq. 12) are the ones previously used (Cupane et al. 1995). Note also that the "old" fitting in terms of Eqs. 6, 7 and 8 (i.e., using the approach by Cupane et al. 1995) corresponds to the $S_j = S = 0$ ($j = 5$–15) value in Eq. 12. As can be seen from Eq. 12, a given mode at frequency ν_j is considered as a high-frequency mode—and therefore contributes to the vibronic progression of Lorentzians—only if $k_B T < h\nu_j c$. At temperatures such that $k_B T > h\nu_j c$ the mode is shifted from the high-frequency to the low-frequency subset, thus contributing to the Gaussian width.
3. The $\sigma^2(T)$ values obtained from the fittings performed in step 2 are analyzed according to

$$\sigma^2(T) = \sigma_{inh}^2 + \sum_j \langle S \rangle f(\nu_j, T) \nu_j^2 coth\left(\frac{h\nu_j}{2k_B T}\right). \quad (13)$$

As already noted, the term σ_{inh} in Eq. 13 takes into account spectral heterogeneity arising from conformational substates; it should also be stressed that the analysis in step 3 does not involve any fitting: indeed, the S value is the same as that used in step 2, while the σ_{inh} value is determined by the fitting of the spectra at low temperatures.

Figure 3 shows fittings of MbCO spectra at $T = 20$ K in terms of Eq. 12, using different values for S; it is evident that the fitting quality depends on S and that $S = 0.00045$ gives a better result than $S = 0.00000$ or $S = 0.00090$. A "cut" of the χ^2 hypersurface parallel to S is reported in Fig. 4 and shows that a minimum is obtained at about $S = 0.0004$, with ± 0.0002 as the 95% confidence interval. The temperature dependence of the Gaussian width (σ^2) obtained by fitting the Soret band in terms of Eq. 12 using various S values is reported in Fig. 5; it shows that, as expected, the σ values depend upon S, the effect being more pronounced at low temperatures. Figure 6 shows the analysis of σ^2 in terms of Eq. 13, at selected S values. The results reported in Fig. 6 deserve some comments:

1. Contrary to what has been reported in previous publications, a σ^2 temperature dependence not obeying the hyperbolic cotangent law is not per se indicative of anharmonicity. Indeed, as clearly shown by the solid lines in Fig. 6, the successive excitation of modes considered in the new model brings about a σ^2 temperature dependence steeper than the simple hyperbolic cotangent behavior.
2. The temperature dependence predicted by the model depends markedly upon the value of S, i.e., upon the coupling of the electronic transition with the vibrational modes. In particular one may have
   a. Anharmonicity (at small S values, where the σ^2 values at high temperatures are above the predicted curve).
   b. Pure harmonic behavior (at $S = 0.00064$, where the σ^2 values overlap with the predicted curve in the

[1]Use of the entire set of low-frequency modes reported in Fig. 2 with a single value for the coupling constant S could, in principle, be questioned. In fact, the density of vibrational states in Fig. 2 has to be "weighted" by the coupling of each mode to the Soret transition. With the Soret transition localized on the heme, only normal modes with a significant eigenvector contribution from the heme macrocycle and/or from atoms in close proximity of the heme should be considered; moreover, in view of the almost planar heme conformation in MbCO, in-plane vibrations are expected to couple much more strongly than out-of-plane vibrations. On the other hand, information on the coupling constants is not directly obtainable from low-frequency Raman spectra, even with Soret excitation, owing to their smallness (weak coupling with a large number of modes). In order to circumvent this difficulty and to check the influence of the previous assumptions on the results of the analyses, we used three different "weighted density of states": (1) the one reported in Fig. 2; (2) a frequency-independent density of states, using the average value of the distribution of Fig. 2; (3) a third distribution of equal area but in which the maximum was shifted to 150 cm^{-1}. The same three distributions were also used for the time domain analysis (see the "Time domain approach" section). For the three distributions the constant S value approximation was used. For all the distributions used the temperature dependence of relevant parameters (i.e., σ^2 for the frequency domain analysis and σ^2_{inh} for the time domain analysis) remained essentially unaltered. We therefore conclude that the assumptions used, although crude, do not alter the main conclusions of the analyses.

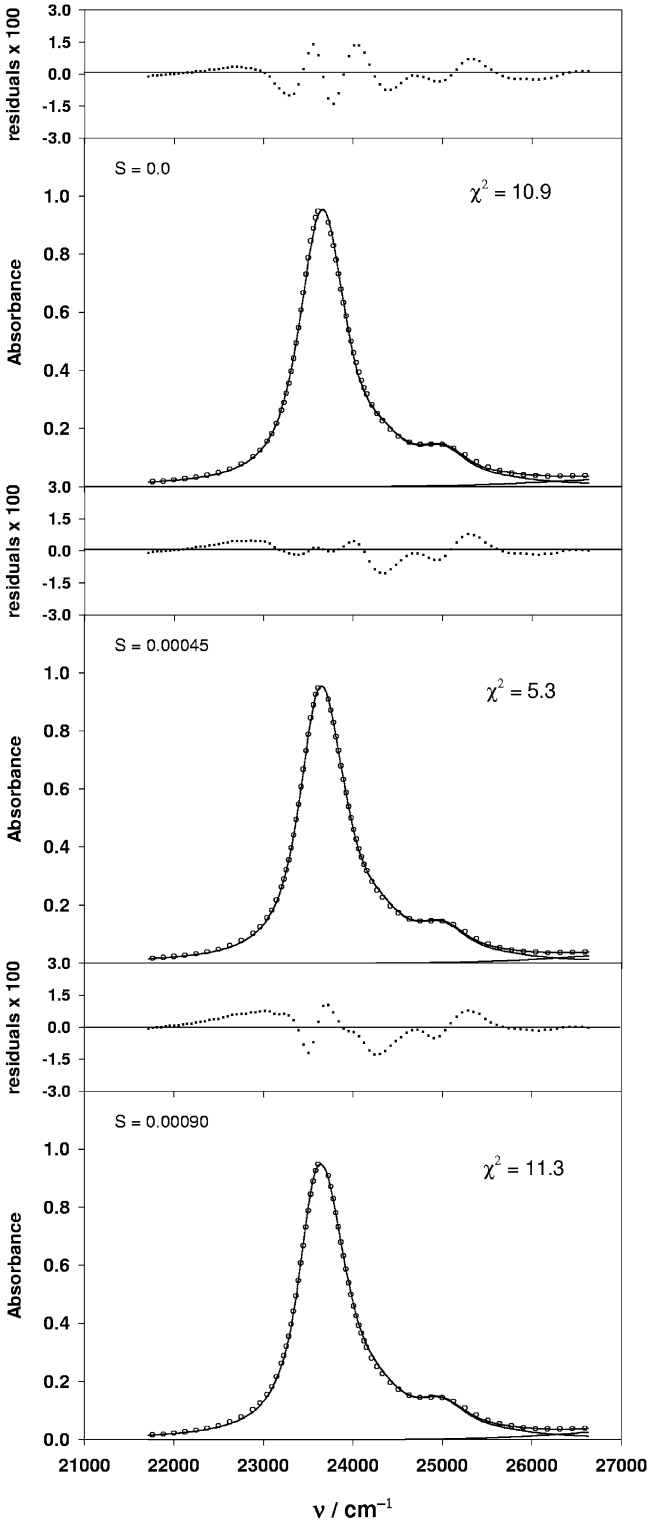

Fig. 3 Soret spectra of MbCO at 20 K. The *circles* are the experimental points (for the sake of readability not all the experimental points have been reported). The *continuous lines* represent the fittings in terms of Eq. 12. Residuals are also reported in the *upper panels* on an expanded scale. The values of S used and of χ^2 obtained are reported in each panel. As usual $\chi^2 = \sum \left[(A_i - A_{i\ \mathrm{calc}})^2 / \Delta^2 \right] / (N - p - 1)$, where N is the number of experimental points, p is the number of fitting parameters and $\Delta = 0.0015$ is the experimental error

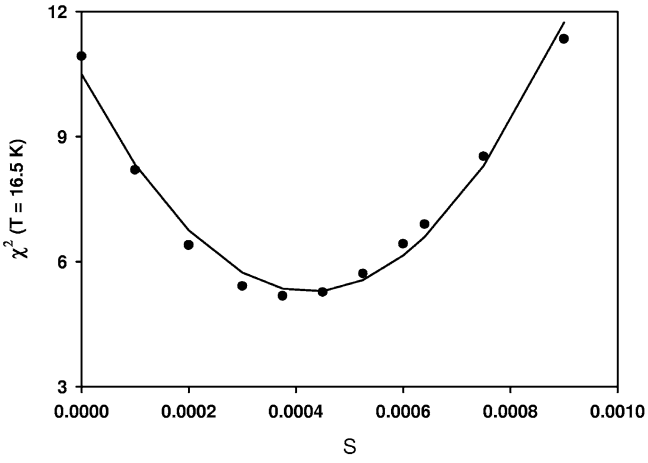

Fig. 4 Cut of the χ^2 hypersurface parallel to S. The *continuous line* is a fitting with a parabola

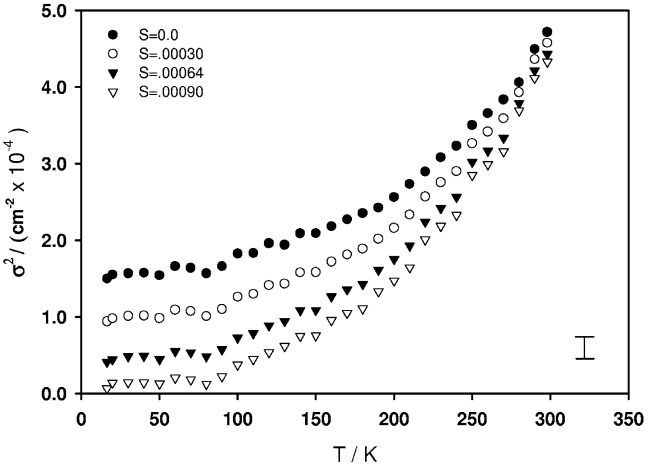

Fig. 5 Temperature dependence of the σ^2 values obtained from spectral fittings performed using different values of S. Different *symbols* refer to different S values. A typical *error bar* is shown

whole temperature range); however, spectral fittings with $S = 0.00064$ are sizably worst than those with $S = 0.00045$ (Figs. 3, 4).

Time domain approach

Spectral analysis in the time domain was performed by using the time correlator of Eqs. 2 and 3 in which the vibrational frequencies and normal modes coupling constants were the same as those used in the "Frequency domain approach" section. Also for the time domain analysis, the three different "weighted densities of vibrational states" described in footnote 1 were used. Integration was performed up to $t_{\max} = 3$ ps using a "Gaussian–Laguerre quadrature" method with 490 integration points. The reliability of the integration method was tested in two ways: (1) by checking

that calculations performed with 810 integration points up to $t_{max} = 5$ ps differed by less than the experimental error (0.001 absorbance units); and (2) by verifying that a time domain analysis of a low-temperature spectrum made by using the time correlator of Eqs. 4 and 5 (short-times approximation) gave the same results as the corresponding frequency domain analysis. In analogy with the frequency domain analysis, only intensity (I), homogeneous width (Γ) and peak frequency (ν_0) were left as free parameters in the spectral fittings.

A fitting of the 20 K MbCO spectrum is shown in the upper panel of Fig. 7; its quality is of the same order as that of the frequency domain fitting (see Fig. 3, middle panel, for comparison). As shown in the lower panel, however, a much better fitting is obtained by inserting in the time correlator of Eq. 3 an additional time decay of the form $\exp(-1/2\sigma^2_{inh}t^2)$; this new term takes into account spectral heterogeneity arising from protein conformational substates. Values of σ_{inh} in the range 50–100 cm^{-1} are obtained, depending on the coupling constant S used; in strict analogy with the frequency domain results (Fig. 4) a minimum in the χ^2 hypersurface is obtained for an S value of 0.00045 with a corresponding σ_{inh} value of 82 cm^{-1} .

In the upper panel of Fig. 8 we report the temperature dependence of σ^2_{inh} obtained using $S = 0.00045$; as can be seen σ^2_{inh} is constant up to about 180 K and then starts increasing with temperature. It should be stressed that fittings of the high-temperature spectra in which σ^2_{inh} was fixed to its low-temperature value gave χ^2 values larger by a factor 3. In close analogy with the frequency domain analysis, the thermal behavior of σ^2_{inh} depends markedly upon the S value (i.e., upon the coupling of the electronic transition with the low-frequency vibrational modes) and decreases with increasing S (Fig. 8, lower panel). In particular, at $S = 0.00064$ the σ^2_{inh} temperature dependence is very weak, indicating almost pure harmonic behavior up to $T = 270$ K. The results in Fig. 8 are consistent with the following picture: at low temperatures the protein is "frozen" in different conformational substates (Austin et al. 1975, Frauenfelder et al. 1988) and protein atoms can perform only harmonic motion within their potential wells and spectral heterogeneity is therefore constant; at high temperatures anharmonic motion sets in and the proteins can explore a larger portion of their energy landscape and an increase of spectral heterogeneity with increasing temperature is observed. The increase of σ^2_{inh} with temperature therefore closely parallels the onset of deviations from the pure harmonic behavior evidenced by the frequency domain analysis (Fig. 6).

Fig. 6 Comparison between the temperature dependence of the σ^2 values obtained from spectral fittings (*circles*) and the σ^2 values calculated using Eq. 13 (*lines*). Different *panels* refer to different values of S. Typical *error bars* are shown

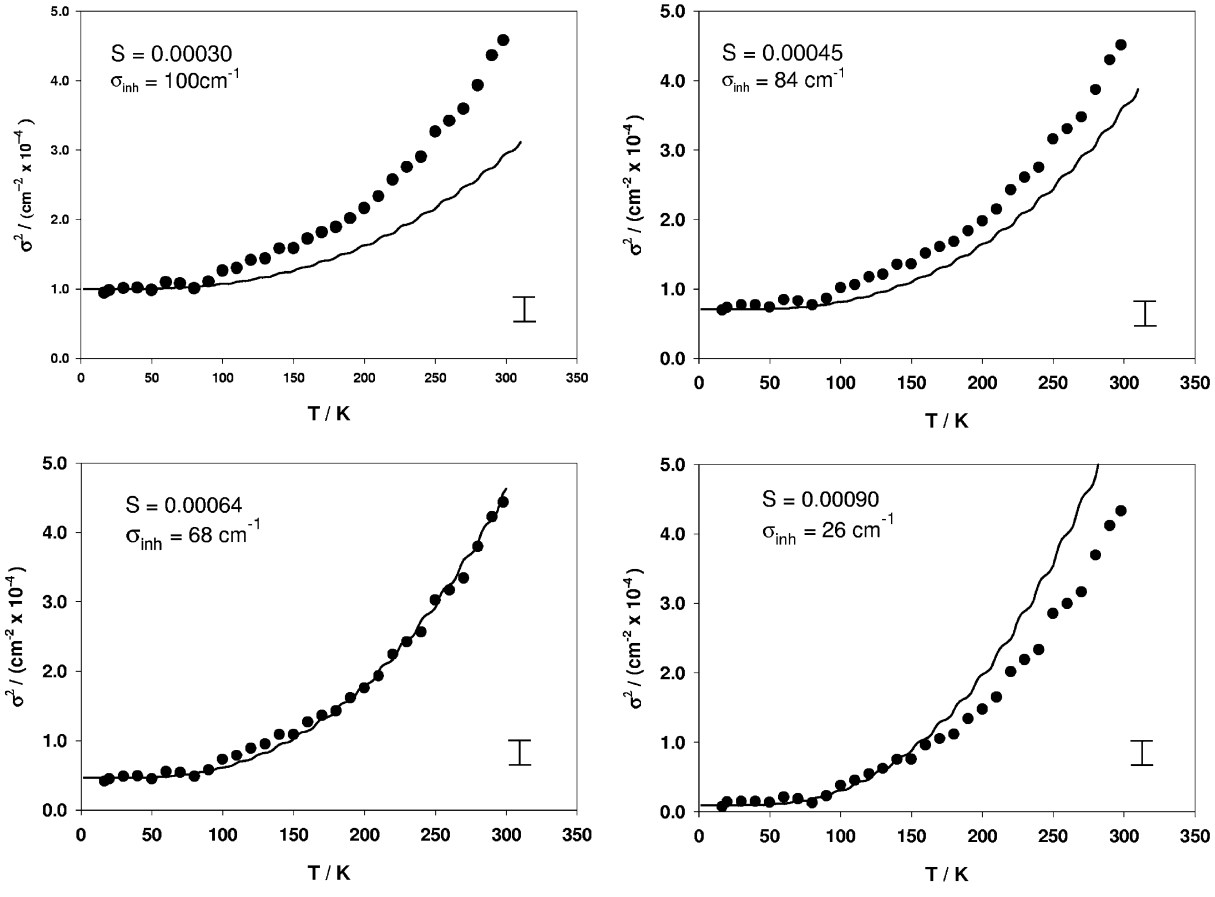

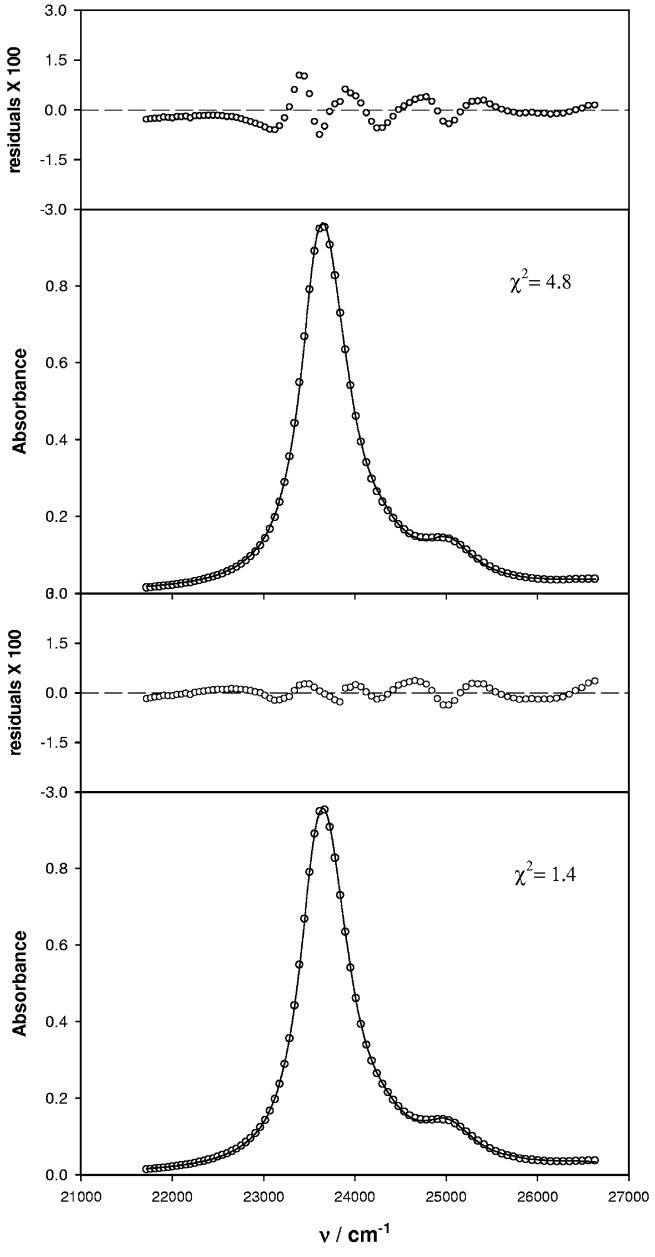

Fig. 7 *Upper panel* Fitting of the 20 K Soret spectrum of MbCO using the time correlator approach (Eqs. 2, 3); *symbols* and residuals as in Fig. 3; for this fitting $S=0.00048$ and $\chi^2=4.9$. *Lower panel* Same as in the *upper panel*, using the modified time correlator (see text); for this fitting $S=0.00048$, $\sigma_{inh}=63\pm3$ cm^{-1} and $\chi^2=1.4$

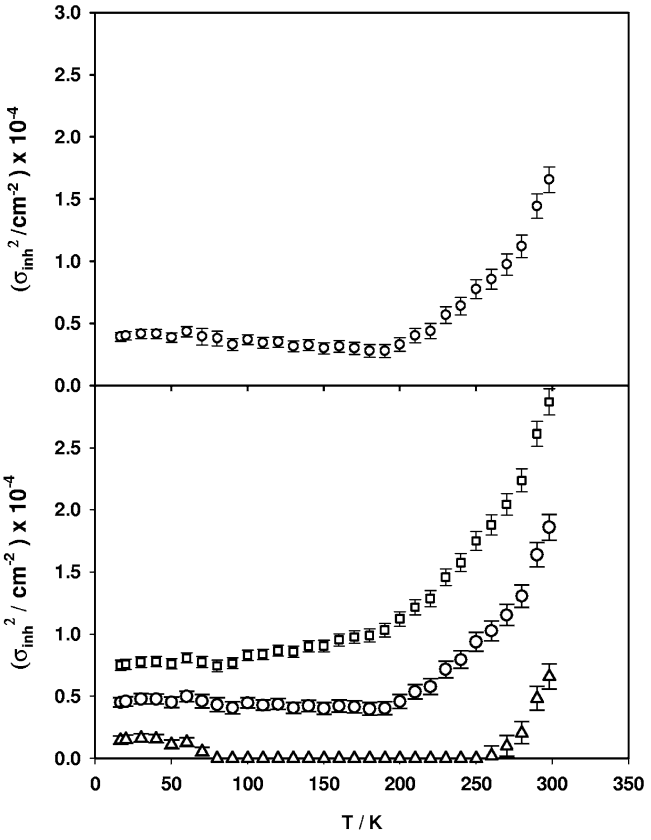

Fig. 8 *Upper panel* Temperature dependence of σ^2_{inh} obtained using $S=0.00045$. *Lower panel* Temperature dependence of σ^2_{inh} at various S values. $S=0.00030$ (*squares*); $S=0.00045$ (*circles*); $S=0.00064$ (*triangles*)

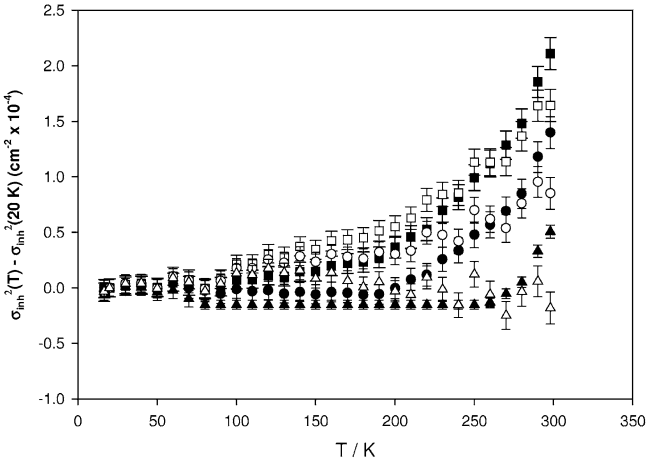

Fig. 9 Anharmonic contributions as a function of temperature. Frequency domain results (*open symbols*); time domain results (*filled symbols*). $S=0.00030$ (*squares*); $S=0.00045$ (*circles*); $S=0.00064$ (*triangles*)

To further highlight the analogy between the time domain and the frequency domain results, in Fig. 9 we report, for different S values, the thermal behavior of $\sigma^2_{inh}(T)-\sigma^2_{inh}(20\text{ K})$ in comparison with $\sigma^2_{anh}(T)$ obtained from the frequency domain results; the quantity $\sigma^2_{anh}(T)$ is defined as the difference between the σ^2 values obtained from spectral fittings in the frequency domain (circles in Fig. 6) and the analogous values calculated using the harmonic approximation, Eq. 13 (lines in Fig. 6). As can be seen, an excellent agreement is obtained; it has to be noted, however, that for $S=0.00064$ the frequency domain analysis predicts harmonic behavior in the whole temperature range 20–300 K ($\sigma^2_{anh}=0$), while the time domain analysis reveals a residual anharmonicity taking place at $T>270$ K.

Conclusions

The results of this work can be summarized as follows:

1. Time domain and frequency domain (modified so as to take properly into account the distinction between high-frequency and low-frequency vibrational modes) analyses give very similar results; in particular they clearly indicate the presence of spectral heterogeneity (σ_{inh}) in the MbCO Soret spectra. It should be emphasized that the departure from harmonicity deduced in the frequency domain analysis from the temperature dependence of σ^2 is replaced in the time domain analysis by a temperature dependence of inhomogeneous broadening (σ^2_{inh}). Within the framework of the conformational substates approach proposed by Frauenfelder and coworkers this implies that at high temperature the protein can "jump" between different conformational substates and this, of course, requires anharmonic motion.
2. The low-temperature value and the thermal behavior of σ_{inh} depend markedly upon the coupling of the Soret band with low-frequency vibrational modes (S).
3. In view of point 2, it is not possible to draw quantitative conclusions about the extent of anharmonicity in the dynamics of the iron with respect to the heme plane in MbCO only from the temperature dependence of the Soret band. In particular, the time domain results (Fig. 8) indicate that, although a temperature dependence of σ^2_{inh} is found with all the S values used, a quantification of its magnitude is difficult at the present stage.
4. Caution should be exerted when comparing optical spectroscopy data with analogous data obtained by other experimental techniques (Parak et al. 1982, Doster et al. 1989); however, since the steepness of the temperature dependence of σ^2 and σ^2_{inh} is highly dependent on the coupling of the electron transition to the low-frequency vibrational modes (Figs. 6, 8), it may be used as a semiquantitative means to compare the dynamic properties of the heme pocket in different states of the protein.

Acknowledgements This work was supported by a grant (COFIN 2000) from the Italian Ministry of Education, University and Research and the Deutsche Forschungsgemeinschaft SFB 433.

References

Austin RH, Beeson KW, Eisenstein L, Frauenfelder H, Gunsalus IC (1975) Dynamics of ligand binding to myoglobin. Biochemistry 14:5355–5373

Bangcharoenpaurpong O, Schomacker KT, Champion PM (1984) A resonance Raman investigation of myoglobin and hemoglobin. J Am Chem Soc 106:5688–5698

Chan CK, Page JB (1983) Temperature effects in the time correlator theory of resonance Raman scattering. J Chem Phys 79:5234–5250

Chan CK, Page JB (1984) T ≠ 0 K Multimode modeling of optical absorption spectra and resonance Raman profiles. Chem Phys Lett 104:609–614

Cupane A, Leone M, Vitrano E, Cordone L (1995) Low temperature optical absorption spectroscopy: an approach to the study of stereodynamic properties of hemeproteins. Eur Biophys J 23:385–398

Cupane A, Leone M, Cordone L, Gilch H, Dreybrodt W, Unger E, Schweitzer-Stenner R (1996) Conformational properties of Nickel(II)–Octaethylporphyrin in solution 2 A low temperature optical absorption spectroscopy study. J Chem Phys 100:14192–14197

Cupane A, Leone M, Unger E, Lemke C, Beck M, Dreybrodt W, Schweitzer-Stenner R (1998) Dynamics of various metal-octaethylporphyrins studied by resonance Raman and low-temperature optical absorption spectroscopies. Role of the central metal. J Phys Chem B102:6612–6620

Di Pace A, Cupane A, Leone M, Vitrano E, Cordone L (1992) Protein dynamics: vibrational coupling, spectral broadening mechanisms and anharmonicity effects in carbonmonoxy heme proteins studied by the temperature dependence of the Soret band lineshape. Biophys J 63:475–484

Doster W, Cusack S, Petry W (1989) Dynamical transition of myoglobin revealed by inelastic neutron scattering. Nature 337:754–756

Frauenfelder H, Parak F, Young RD (1988) Conformational substates in proteins. Annu Rev Biophys Biophys Chem 17:451–459

Leone M, Cupane A, Militello V, Cordone L (1994) Thermal broadening of the Soret band in heme complexes and in heme proteins: role of the iron dynamics. Eur Biophys J 23:349–352

Melchers B, Knapp EW, Parak F, Cordone L, Cupane A, Leone M (1996) Structural fluctuations of myoglobin from normal modes, Mössbauer, Raman and absorption spectroscopy. Biophys J 70:2092–2099

Parak F, Knapp EW, Kucheida D (1982) Protein dynamics. Mossbauer spectroscopy on deoxymyoglobin crystals. J Mol Biol 161:177–194

Schomacker KT, Champion PM (1986) Investigations of spectral broadening mechanisms in biomolecules: Cytochrome-c. J Chem Phys 84:5314–5325

Schweitzer-Stenner R, Bigman D (2001) Electronic and vibronic contributions to the band splitting in optical spectra of heme proteins. J Chem Phys B 105:7064–7073

Srajer V, Schomacker KT, Champion PM (1986) Spectral broadening in biomolecules. Phys Rev Lett 57:1267–1270